$W_2Cl_4(NR_2)_2(PR'_3)_2$ Molecules. 5. Preparation and Characterization of $W_2Cl_4(NEt_2)_2$(L-L) (L-L = dmpm, dmpe, dppe), $W_2Cl_4(NBu_2)_2$(L-L) (L-L = dmpm, dmpe), and $W_2Cl_4(NHex_2)_2$(dmpm). First Complexes with Bridging Diphosphine Ligands in a *cis,trans*-Stereochemistry

F. Albert Cotton,* Evgeny V. Dikarev, and Wai-Yeung Wong

Department of Chemistry and Laboratory for Molecular Structure and Bonding, Texas A&M University, College Station, Texas 77843-3255

Received September 18, 1996[⊗]

The triply-bonded ditungsten complexes $W_2Cl_4(NEt_2)_2$(L-L) (L-L = dmpm, dmpe), $W_2Cl_4(NBu_2)_2$(L-L) (L-L = dmpm, dmpe), and $W_2Cl_4(NHex_2)_2$(dmpm) are formed in the reactions between $W_2Cl_4(NR_2)_2(NHR_2)_2$ (R = Et, Bu, Hex = *n*-C_6H_{13}) and bis(dimethylphosphino)methane (dmpm) or bis(dimethylphosphino)ethane (dmpe). In each case, three isomeric forms have been detected in solution by $^{31}P\{^1H\}$ NMR spectroscopy, and they are formulated as the *trans,trans*-, *cis,trans*-, and *cis,cis*-isomers. Complexes designated cis,trans have one P atom of the bridging diphosphine cis to the N atom on one W atom and another P atom trans to the N atom on the other W atom. The characterization of *cis,trans*-$W_2Cl_4(NEt_2)_2$(dmpm) (**1**), *cis,cis*-$W_2Cl_4(NEt_2)_2$(dmpm) (**2**), *cis,trans*-$W_2Cl_4(NBu_2)_2$(dmpm) (**3**), *cis,cis*-$W_2Cl_4(NBu_2)_2$(dmpm) (**4a**, **4b**), *cis,cis*-$W_2Cl_4(NHex_2)_2$(dmpm) (**5**), *cis,trans*-$W_2Cl_4(NEt_2)_2$(dmpe) (**6**), and *cis,trans*-$W_2Cl_4(NBu_2)_2$(dmpe) (**7**) has been accomplished by X-ray crystallography. Pertinent crystal data are as follows: for **1**, monoclinic space group *C*2/*c*, $a = 33.210(3)$ Å, $b = 8.725(4)$ Å, $c = 17.052(4)$ Å, $\beta = 100.44(1)°$, $Z = 8$; for **2**, monoclinic space group $P2_1/c$, $a = 8.760(3)$ Å, $b = 21.028(8)$ Å, $c = 12.778(5)$ Å, $\beta = 91.77(3)°$, $Z = 4$; for **3**, orthorhombic space group *Pbca*, $a = 14.958(2)$ Å, $b = 15.823(2)$ Å, $c = 27.8014(9)$ Å, $Z = 8$; for **4a**, *C*2/*c*, $a = 18.011(4)$ Å, $b = 17.221(4)$ Å, $c = 21.264(6)$ Å, $\beta = 103.33(2)°$, $Z = 8$; for **4b** (**4a,b** are polymorphic), *Pbca*, $a = 14.772(2)$ Å, $b = 17.188(1)$ Å, $c = 25.370(3)$ Å, $Z = 8$; for **5**, *C*2/*c*, $a = 18.368(4)$ Å, $b = 17.060(2)$ Å, $c = 30.414(4)$ Å, $\beta = 103.96(1)°$, $Z = 8$; for **6**, $P2_1/c$, $a = 9.596(2)$ Å, $b = 15.975(2)$ Å, $c = 18.756(4)$ Å, $\beta = 96.73(1)°$, $Z = 4$; for **7**, monoclinic space group $P2_1/n$, $a = 9.465(1)$ Å, $b = 34.545(7)$ Å, $c = 10.177(4)$ Å, $\beta = 97.220(1)°$, $Z = 4$. Among them is one unprecedented type of geometrical isomer, namely, the *cis,trans*-isomers of $W_2Cl_4P_2N_2$ complexes. In order to structurally characterize a *trans,trans*-isomer for $W_2Cl_4(NR_2)_2$(L-L) molecules, a bis(diphenylphosphino)ethane (dppe) analogue, *trans,trans*-$W_2Cl_4(NEt_2)_2$(dppe) (**8**), has been prepared, and it crystallizes with a molecule of toluene, in the space group $P2_1/n$ with $a = 16.396(3)$ Å, $b = 10.104(2)$ Å, $c = 26.680(2)$ Å, $\beta = 92.22(1)°$, and $Z = 4$. Each of the compounds **1**−**8** has an essentially staggered $W_2Cl_4P_2N_2$ conformation with the W atoms bound by a triple bond. The W−W distances fall within the narrow range 2.314−2.341 Å. All of them show significant torsion angles in the solid state.

Introduction

The recent syntheses of $W_2Cl_4(NHCMe_3)_2$(L-L) (L-L = dmpm, dmpe, dppm, dppe)[1] and $W_2Cl_4(NR_2)_2(PR'_3)_2$ (R = Et, Bu, Hex; R′$_3$= Me_3, Et_2H)[2] molecules sparked our interest for the preparation of a new type of complex having the stoichiometry $W_2Cl_4(NR_2)_2$(L-L), where L-L is a bidentate phosphine. We therefore undertook studies of the reaction of $W_2Cl_4(NR_2)_2(NHR_2)_2$ with some diphosphine ligands.

There are six distinct geometric isomers for d^3-d^3 complexes with a $W_2Cl_4P_2N_2$ core in a staggered geometry (where P_2 is a bridging diphosphine), as illustrated in Figure 1. They are *trans,trans*- (I), two types of *cis,trans*- (II and III) and three types of *cis,cis*- (IV−VI) isomers. None of these geometrical isomers has ever been reported, though examples of *cis,cis*-$W_2Cl_4(NHCMe_3)_2$(L-L) (L-L = diphosphines) in a partly eclipsed geometry[1] and *trans,trans*- and *cis,cis*-$W_2Cl_4(NHCMe_3)_2(PMe_3)_2$ in a perfect eclipsed geometry[3] are known in the literature. One type I complex, three type IV complexes, and four complexes of the unprecedented type II have now been prepared and structurally characterized. The present work is also an interesting extension of the earlier studies on $W_2Cl_4(NHCMe_3)_2$(L-L) and $W_2Cl_4(NR_2)_2(PR'_3)_2$ type compounds.

Experimental Section

General Procedures. All manipulations were carried out under an atmosphere of dinitrogen or argon. Standard Schlenk and vacuum line techniques were used. Toluene, hexanes, and THF were purified by distillation under N_2 from potassium/sodium benzophenone ketyl. Dichloromethane was distilled under N_2 from phosphorus pentoxide. dmpm and dmpe were purchased from Strem Chemicals and used as received. All dialkylamines and dppe were purchased from Aldrich, Inc., and used without further purification. WCl_4 was prepared by refluxing WCl_6 and $W(CO)_6$ in chlorobenzene,[4] and $W_2Cl_6(THF)_4$ was prepared according to the literature method using Na−Hg as the reducing agent.[5]

Syntheses. (i) $W_2Cl_4(NEt_2)_2$(dmpm). An excess of dmpm (0.12 mL) was added by syringe to a stirred solution of $W_2Cl_4(NEt_2)_2(NHEt_2)_2$

⊗ Abstract published in *Advance ACS Abstracts*, February 1, 1997.

(1) Cotton, F. A.; Dikarev, E. V.; Wong, W. Y. *Inorg. Chem.* **1997**, *36*, 80.
(2) Cotton, F. A.; Dikarev, E. V.; Nawar, N.; Wong, W. Y. *Inorg. Chem.* **1997**, *36*, 559.
(3) (a) Bradley, D. C.; Hursthouse, M. B.; Powell, H. R. *J. Chem. Soc., Dalton Trans.* **1989**, 1537. (b) Cotton, F. A.; Yao, Z. *J. Cluster Sci.* **1994**, *5*, 11.
(4) Schrock, R. R.; Sturgeoff, L. G.; Sharp, P. R. *Inorg. Chem.* **1983**, *22*, 2801.

S0020-1669(96)01151-2 CCC: $14.00

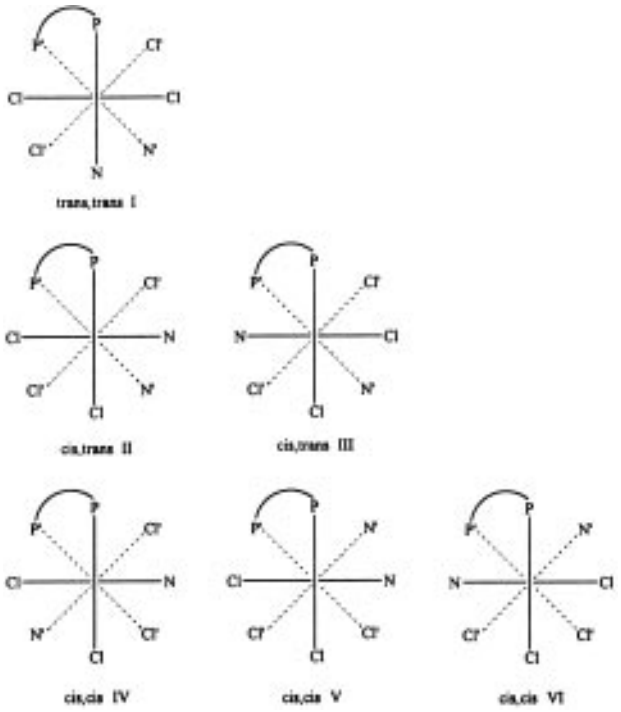

Figure 1. The six possible geometrical isomers for $W_2Cl_4(NR_2)_2$(L-L) molecules.

prepared by reaction of $W_2Cl_6(THF)_4$ (from 0.50 g of WCl_4) with diethylamine in tetrahydrofuran (15 mL).[2] The solution started to turn dark-brown, and *in situ* monitoring by $^{31}P\{^1H\}$ NMR spectroscopy of a sample of the mixture at the very beginning of the experiment (within 10 min) showed the presence of *trans*,*trans*- and *cis*,*trans*-isomers in the approximate proportion 72:28, respectively, based on integrated intensities of the $^{31}P\{^1H\}$ NMR spectral peaks at room temperature. As time passed, three isomers corresponding to *trans*,*trans*-, *cis*,*trans*- and *cis*,*cis*-stereochemistry appeared at the same time in the mixture. After about 1 h of stirring, the solvent and other volatile components were removed under vacuum. The residual solid was redissolved in hot toluene (10 mL) to give a deep red solution, and 15 mL of hexanes was layered on it. Bright red microcrystalline *cis*,*cis*-$W_2Cl_4(NEt_2)_2$(dmpm) (**2**) (0.35 g, 58% based on WCl_4) and a tiny amount of dark-red crystals of *cis*,*trans*-$W_2Cl_4(NEt_2)_2$(dmpm) (**1**) (24 mg, 4%) were observed in the Schlenk tube after 1 day at room temperature. Attempts to isolate and crystallize the *trans*,*trans*-isomer were unsuccessful so far, and no attempts were made to optimize the yield of **1** in this reaction. Single crystals of **2** were obtained by slow diffusion of hexanes into a solution of **2** in dichloromethane at room temperature for 2 days.

For the *trans*,*trans*-isomer, $^{31}P\{^1H\}$ NMR data (C_6D_6 + THF, 19 °C, δ): −1.74(s, $^1J_{W-P}$ = 57 Hz, $^2J_{P-P}$ = 13.0 Hz).

For **1**, $^{31}P\{^1H\}$ NMR data (C_6D_6 + THF, 19 °C, δ): −0.45 (d, $^2J_{P-P}$ = 101.8 Hz, trans-P), 2.68 (d, $^2J_{P-P}$ = 101.8 Hz, cis-P).

For **2**, IR data (cm^{-1}): 1409 (w), 1366 (ms), 1354 (m), 1294 (w), 1284 (m), 1261 (s), 1185 (w), 1153 (w), 1144 (w), 1099 (s), 1080 (s), 1018 (s), 1007 (s), 950 (ms), 935 (s), 895 (vw), 879 (w), 873 (w), 845 (w), 803 (vs), 747 (w).

^1H NMR data ($CDCl_3$, 24 °C, δ): 0.98 (t, J = 7.1 Hz, 6H, distal CH_3), 1.46 (t, J = 7.1 Hz, 6H, proximal CH_3), 1.49 (t, J = 4.8 Hz, 6H, PMe_2), 2.23 (t + m, J = 4.8 Hz, 8H, PMe_2 + distal NCH_2CH_3), 2.74 (m, 2H, distal NCH_2CH_3), 3.70 (t, J = 10.6 Hz, 2H, PCH_2P), 4.37 (m, 2H, proximal NCH_2CH_3), 6.28 (m, 2H, proximal NCH_2CH_3).

$^{31}P\{^1H\}$ NMR data (C_6D_6 + THF, 19 °C, δ): 5.86 (s, $^1J_{W-P}$ = 150 Hz, $^2J_{P-P}$ = 76.7 Hz).

FAB/DIP (NBA, CH_2Cl_2, *m/z*): 790 ($[M]^+$), 755 ($[M - Cl]^+$), 718 ($[M - 2Cl]^+$ or $[M - NEt_2]^+$), 681 ($[M - 3Cl]^+$ or $[M - Cl - NEt_2]^+$).

(5) (a) Chisholm, M. H.; Eichhorn, B. W.; Folting, K.; Huffman, J. C.; Ontiveros, C. D.; Streib, W. E.; Van Der Sluys, W. G. *Inorg. Chem.* **1987**, *26*, 3182. (b) Sharp, P. R.; Schrock, R. R. *J. Am. Chem. Soc.* **1980**, *102*, 1430.

(ii) $W_2Cl_4(NBu_2)_2$(dmpm). To the tetrahydrofuran solution (15 mL) of $W_2Cl_4(NBu_2)_2(NHBu_2)_2$ (from 0.50 g WCl_4)[2] was added excess dmpm (0.12 mL) via syringe, and the color of the solution became dark-brown in a few minutes. As in (i), the $^{31}P\{^1H\}$ NMR spectrum of this solution mixture again indicated that three distinct isomers of $W_2Cl_4(NBu_2)_2$(dmpm) were present. The reaction mixture was stirred for about 1 h, after which all the volatile components were removed under vacuum. The dark red-brown residue was first extracted with warm hexanes (10 mL), from which some tiny red crystals of **3** of good X-ray quality (40 mg, 6%) were obtained by keeping the hexanes extract in a freezer at ca. −15 °C for several days. No attempts were made to optimize the yield of **3** in this reaction. The remaining residue was then redissolved in hot toluene (15 mL), and isomeric hexanes was carefully layered on this deep red solution. This layered mixture was left undisturbed for 1 week, producing *cis*,*cis*-$W_2Cl_4(NBu_2)_2$(dmpm) (**4a,b**) in two polymorphic forms with the overall yield of about 52%, based on WCl_4.

For the *trans*,*trans*-isomer, $^{31}P\{^1H\}$ NMR data (C_6D_6 + toluene + THF, 19 °C, δ): −3.15 (s, $^1J_{W-P}$ = 56 Hz, $^2J_{P-P}$ = 12.2 Hz).

For **3**, $^{31}P\{^1H\}$ NMR data (C_6D_6 + toluene + THF, 19 °C, δ): −1.06 (d, $^2J_{P-P}$ = 101.4 Hz, trans-P), 1.56 (d, $^2J_{P-P}$ = 101.4 Hz, cis-P).

For **4**, IR data (cm^{-1}): 1414 (w), 1296 (w), 1283 (w), 1261 (vs), 1171 (w), 1094 (vs, br), 1020 (vs, br), 957 (m), 940 (m), 901 (w), 872 (w), 853 (w), 801 (vs), 744 (w).

^1H NMR data (C_6D_6, 24 °C, δ): 0.88−0.96 (m, 10H, distal CH_3 + $NCH_2(CH_2)_2CH_3$), 1.05−1.22 (m, 20H, proximal CH_3 + PMe_2 + $NCH_2(CH_2)_2CH_3$), 1.67 (m, br, 4H, $NCH_2(CH_2)_2CH_3$), 1.90 (virtual t, 6H, PMe_2), 2.18 (m, 2H, distal $NCH_2(CH_2)_2CH_3$), 2.72 (m, 2H, distal $NCH_2(CH_2)_2CH_3$), 2.91 (t, J = 10 Hz, 2H, PCH_2P), 4.13 (m, 2H, proximal $NCH_2(CH_2)_2CH_3$), 6.75 (m, 2H, proximal $NCH_2(CH_2)_2CH_3$).

$^{31}P\{^1H\}$ NMR data (C_6D_6 + toluene + THF, 19 °C, δ): 4.73 (s, $^1J_{W-P}$ = 150 Hz, $^2J_{P-P}$ = 74.9 Hz).

FAB/DIP (NBA, neat, *m/z*): 902 ($[M]^+$), 866 ($[M - Cl]^+$), 774 ($[M - NBu_2]^+$), 738 ($[M - 2Cl]^+$), 646 ($[M - 2NBu_2]^+$).

(iii) $W_2Cl_4(NHex_2)_2$(dmpm). The synthesis of $W_2Cl_4(NHex_2)_2$(dmpm) followed a similar course to that for (i) and (ii). Upon addition of dmpm to a solution of $W_2Cl_4(NHex_2)_2(NHHex_2)_2$ (from 0.50 g of WCl_4) in tetrahydrofuran (15 mL),[2] the $^{31}P\{^1H\}$ NMR spectrum initially revealed a mixture of *trans*,*trans*- and *cis*,*cis*-isomers in solution in ratio of 76:24 after 10 min at room temperature. After 1 h of stirring, all the volatile components of the slurry were removed under reduced pressure. Initial hexanes extraction (15 mL) of the resulting residue led to immediate crystallization of irregular orange-red microcrystals of **5** at room temperature as identified by $^{31}P\{^1H\}$ NMR spectroscopy. The residue was extracted with a minimum volume of toluene (10 mL), and hexanes were layered on this solution. However, no crystals were obtained in this way. A second crop of red crystals of **5** suitable for X-ray diffraction studies was then obtained from the toluene/hexanes solvent mixture at −15 °C after 1 week. The overall yield of **5** was about 55%, based on starting WCl_4. However, no crystals were yet available for the other two isomers.

For the *trans*,*trans*-isomers, $^{31}P\{^1H\}$ NMR data (C_6D_6 + THF, 19 °C, δ): −2.00 (s, $^1J_{W-P}$ = 57 Hz, $^2J_{P-P}$ = 13.0 Hz).

For the *cis*,*trans*-isomer, $^{31}P\{^1H\}$ NMR data (C_6D_6 + THF, 19 °C, δ): −0.32 (d, $^2J_{P-P}$ = 101.4 Hz, trans-P), 2.76 (d, $^2J_{P-P}$ = 101.4 Hz, cis-P).

For **5**, IR data (cm^{-1}): 1418 (w), 1296 (w), 1282 (w), 1260 (s), 1150 (w), 1092 (s, br), 1019 (s, br), 957 (m), 938 (m), 873 (w), 799 (vs).

^1H NMR data (C_6D_6, 24 °C, δ): 0.76 (virtual t, 6H, distal CH_3), 0.91 (m, 14H, proximal CH_3 + $NCH_2(CH_2)_4CH_3$), 1.10(virtual t, J = 3.9 Hz, 6H, PMe_2), 1.13−1.60 (m, br, 16H, $NCH_2(CH_2)_4CH_3$), 1.92 (virtual t, J = 4.7 Hz, 6H, PMe_2), 2.23 (m, 2H, distal $NCH_2(CH_2)_4CH_3$), 2.50 (m, 8H, $NCH_2(CH_2)_4CH_3$), 2.80 (m, 2H, distal $NCH_2(CH_2)_4CH_3$), 2.94 (t, J = 10.5 Hz, 2H, PCH_2P), 4.18 (m, 2H, proximal $NCH_2(CH_2)_4CH_3$), 6.75 (m, 2H, proximal $NCH_2(CH_2)_4CH_3$).

$^{31}P\{^1H\}$ NMR data (C_6D_6 + THF, 19 °C, δ): 5.74 (s, $^1J_{W-P}$ = 149 Hz, $^2J_{P-P}$ = 76.2 Hz).

FAB/DIP (NBA, neat, *m/z*): 1014 ($[M]^+$), 978 ($[M - Cl]^+$), 830 ($[M - NHex_2]^+$), 794 ($[M - Cl - NHex_2]^+$).

(iv) $W_2Cl_4(NEt_2)_2$(dmpe). Similar procedures to those for (i) were followed to prepare $W_2Cl_4(NEt_2)_2$(dmpe) using dmpe (0.13 mL, >1

equiv) instead of dmpm. The reaction mixture immediately after mixing of the reactants was shown by $^{31}P\{^1H\}$ NMR spectroscopy to contain a mixture of *trans,trans*-, *cis,trans*-, and *cis,cis*-isomers in the approximate proportion 75:24:1. Stirring was continued for 1 h, after which the solvent and other volatile components were removed *in vacuo*. The residue was then extracted with warm hexanes (20 mL), and the bright red solution was concentrated and allowed to stand at room temperature for 3−4 days to afford a first crop of red plate-shaped crystals of *trans,trans*-$W_2Cl_4(NEt_2)_2$(dmpe) as identified by $^{31}P\{^1H\}$ NMR spectroscopy and mass spectrometry. A second crop of red crystals was obtained by keeping the supernatant liquid at 0 °C for 2 days. The overall yield was about 51%. In fact, X-ray data collection has been carried out for these crystals four times and each case led to an orthorhombic or tetragonal crystal system. However, attempts to solve the structure have met with little success, probably due to the occurrence of superlattices for the crystals. The remaining residue was dissolved in toluene (10 mL) to give an orange-red solution. Orange-red crystalline solids of **6** (0.11 g, 18%) were obtained upon cooling a concentrated toluene solution to 0 °C for 2−3 days. Single crystals of **6** were grown by slow diffusion of hexanes into a dichloromethane solution of **6** at room temperature for 2 days, but slight decomposition also took place to leave some brown precipitates. Following toluene extraction, the remaining residue was further dissolved in CH_2Cl_2. The $^{31}P\{^1H\}$ spectrum of this CH_2Cl_2 solution shows a significant amount of *cis,cis*-$W_2Cl_4(NEt_2)_2$(dmpe), but this complex readily undergoes oxidation in chlorinated solvents at ambient temperature.

The same reaction has also been carried out using a pure crystalline sample of *cis,cis*-$W_2Cl_4(NEt_2)_2(NHEt_2)_2$, and the results were essentially the same.

For the *trans,trans*-isomer, IR data (cm^{-1}): 1417 (w), 1356 (vw), 1300 (w), 1282 (w), 1261 (vs), 1185 (vw), 1148 (sh), 1095 (vs), 1019 (vs), 946 (m), 935 (w), 880 (m), 869 (sh), 799 (vs), 740 (vw), 668 (vw), 644 (vw).

^1H NMR data (C_6D_6, 24 °C, δ): 0.78 (d, $J = 8.9$ Hz, 6H, PMe_2), 1.01 (m, 8H, distal $CH_3 + CH_2$ protons of $Me_2P(CH_2)_2PMe_2$), 1.48 (t, $J = 7.1$ Hz, 6H, proximal CH_3), 1.67 (d, $J = 9.2$ Hz, 6H, PMe_2), 2.03 (d, $J = 9.2$ Hz, 2H, CH_2 protons of $Me_2P(CH_2)_2PMe_2$), 2.59 (m, 2H, distal NCH_2CH_3), 2.92 (m, 2H, distal NCH_2CH_3), 4.66 (m, 2H, proximal NCH_2CH_3), 5.87 (m, 2H, proximal NCH_2CH_3).

$^{31}P\{^1H\}$ NMR data (C_6D_6, 19 °C, δ): 6.14 (s, $^1J_{W-P} = 112$ Hz, $^3J_{P-P} = 23.0$ Hz).

FAB/DIP (NBA, C_6H_6, *m/z*): 804 ($[M]^+$), 769 ($[M - Cl]^+$), 733 ($[M - 2Cl]^+$ or $[M - NEt_2]^+$), 695 ($[M - 3Cl]^+$ or $[M - Cl - NEt_2]^+$), 660 ($[M - 2Cl - NEt_2]^+$).

For **6**, IR data (cm^{-1}): 1494 (w), 1418 (m), 1354 (m), 1300 (m), 1284 (m), 1261 (w), 1183 (w), 1158 (vw), 1144 (w), 1097 (m), 1066 (w), 1038 (w), 1023 (vw), 1000 (ms), 947 (vs), 931 (s), 894 (w), 883 (m), 841 (w), 797 (s), 744 (m), 733 (ms), 714 (ms), 696 (w), 644 (m).

^1H NMR data ($CDCl_3$, 24 °C, δ): 1.05−1.23 (m), 1.31−1.54 (m), 1.82 (d, $J = 9.4$ Hz, 3H, PMe_2), 1.97 (d, $J = 9.4$ Hz, 3H, PMe_2), 2.30−3.08 (m, br, distal NCH_2CH_3), 4.77 (m, 1H, proximal NCH_2CH_3), 5.03 (m, 1H, proximal NCH_2CH_3), 5.26 (m, 1H, proximal NCH_2CH_3), 5.92 (m, 1H, proximal NCH_2CH_3).

$^{31}P\{^1H\}$ NMR data (C_6D_6, 19 °C, δ): 5.58 (d, $^1J_{W-P} = 141$ Hz, $^3J_{P-P} = 32.5$ Hz, trans-P), 8.92 (d, $^1J_{W-P} = 292$ Hz, $^3J_{P-P} = 32.5$ Hz).

FAB/DIP (NBA, neat, *m/z*): 804 ($[M]^+$), 769 ($[M\text{-}Cl]^+$), 733 ($[M - 2Cl]^+$ or $[M - NEt_2]^+$), 695 ($[M - 3Cl]^+$ or $[M - Cl - NEt_2]^+$).

For the *cis,cis*-isomer, $^{31}P\{^1H\}$ NMR data (C_6D_6 + toluene, 19 °C, δ): 10.42 (s, $^1J_{W-P} = 303$ Hz, $^3J_{P-P} = 47.5$ Hz).

(v) $W_2Cl_4(NBu_2)_2$(dmpe). Compound $W_2Cl_4(NBu_2)_2$(dmpe) was prepared in a similar manner as $W_2Cl_4(NEt_2)_2$(dmpe) using $W_2Cl_4(NBu_2)_2(NHBu_2)_2$ as the starting material instead. Upon the addition of dmpe (0.13 mL) and with similar work−up procedures using extraction into hexanes (20 mL), an abundant crop of red crystals of *trans,trans*-$W_2Cl_4(NBu_2)_2$(dmpe) (0.40 g, 57%) was obtained by cooling a concentrated hexanes solution to ca. 0 °C for 1 week. As for the analogous *trans,trans*-$W_2Cl_4(NEt_2)_2$(dmpe) complex, no structure solution has yet been available for these crystals. When hexanes were layered on the toluene extract of the remaining residue, plate-shaped orange-red crystals of **7** (71 mg, 10%) formed in 2 days at room temperature. Attempts to isolate the *cis,cis*-isomer are so far unsuccessful.

For the *trans,trans*-isomer, IR data (cm^{-1}): 1419 (s), 1363 (m), 1300 (ms), 1284 (ms), 1260 (w), 1225 (vw), 1156 (ms), 1115 (m), 1106 (m), 1074 (m), 1051 (vw), 1018 (m), 998 (ms), 952 (vs), 934 (vs), 916 (vs), 897 (s), 882 (w), 872 (vw), 844 (ms), 808 (w), 796 (m), 780 (w), 742 (s), 711 (s), 643 (s).

^1H NMR data (C_6D_6, 24 °C, δ): 0.79 (d, $J = 6.8$ Hz, 6H, PMe_2), 0.82 (t, $J = 7.2$ Hz, 6H, distal CH_3), 1.07 (t, $J = 7.2$ Hz, 6H, proximal CH_3), 1.23 (m, $NCH_2(CH_2)_4CH_3$ and part of CH_2 protons of $Me_2P(CH_2)_2PMe_2$), 1.67 (d, $J = 9.2$ Hz, 6H, PMe_2), 1.50−1.88 (m, br, $NCH_2(CH_2)_4CH_3$), 2.04 (d, $J = 10.4$ Hz, CH_2 protons of $Me_2P(CH_2)_2PMe_2$), 2.57 (m, 2H, distal $NCH_2(CH_2)_4CH_3$), 3.10 (m, 2H, distal $NCH_2(CH_2)_4CH_3$), 4.77 (m, 2H, proximal $NCH_2(CH_2)_4CH_3$), 5.98 (m, 2H, proximal $NCH_2(CH_2)_4CH_3$).

$^{31}P\{^1H\}$ NMR data (C_6D_6, 19 °C, δ): 6.16 (s, $^1J_{W-P} = 112$ Hz, $^3J_{P-P} = 23.0$ Hz).

FAB/DIP (NBA, C_6H_6, *m/z*): 916 ($[M]^+$), 881 ($[M - Cl]^+$), 788 ($[M - NBu_2]^+$), 751 ($[M - Cl - NBu_2]^+$), 716 ($[M - 2Cl - NBu_2]^+$), 661 ($[M - 2NBu_2]^+$).

For **7**, IR data (cm^{-1}): 1422 (vw), 1412 (vw), 1383 (m), 1303 (w), 1285 (w), 1261 (ms), 1160 (w), 1095 (s), 1020 (s), 947 (m), 934 (m), 918 (w), 900 (w), 875 (vw), 801 (s), 744 (w), 715 (w), 667 (vw), 643 (vw).

^1H NMR data ($CDCl_3$, 24 °C, δ): 0.83 (m), 0.93−1.27 (m), 1.36−1.61 (m), 1.82 (d, $J = 8.8$ Hz, 3H, PMe_2), 1.97 (d, $J = 8.8$ Hz, 3H, PMe_2), 2.08−2.99 (m, distal $NCH_2(CH_2)_4CH_3$), 4.59 (m, 1H, proximal $NCH_2(CH_2)_4CH_3$), 4.90 (m, 1H, proximal $NCH_2(CH_2)_4CH_3$), 5.20 (m, 1H, proximal $NCH_2(CH_2)_4CH_3$), 5.89 (m, 1H, proximal $NCH_2(CH_2)_4CH_3$).

$^{31}P\{^1H\}$ NMR data (C_6D_6, 19 °C, δ): 6.03 (d, $^1J_{W-P} = 140$ Hz, $^3J_{P-P} = 32.7$ Hz, trans-P), 9.34 (d, $^1J_{W-P} = 293$ Hz, $^3J_{P-P} = 32.7$ Hz, cis-P).

FAB/DIP (NBA, neat, *m/z*): 916 ($[M]^+$), 881 ($[M - Cl]^+$), 788 ($[M - NBu_2]^+$), 751 ($[M - Cl - NBu_2]^+$), 660 ($[M - 2NBu_2]^+$).

For the *cis,cis*-isomer, $^{31}P\{^1H\}$ NMR data (C_6D_6 + toluene, 19 °C, δ): 10.74 (s, $^1J_{W-P} = 303$ Hz, $^3J_{P-P} = 45.9$ Hz).

(vi) *trans,trans*-$W_2Cl_4(NEt_2)_2$(dppe) (8). dppe (0.30 g, >1 equiv) was dissolved in toluene (5 mL) and added via cannula to a solution of $W_2Cl_4(NEt_2)_2(NHEt_2)_2$ prepared *in situ* from 0.50 g of WCl_4 in tetrahydrofuran (15 mL). The $^{31}P\{^1H\}$ NMR spectrum of the reaction mixture indicated that compound **8** was the sole product (as identified by X-ray diffraction) and no other isomers were observed even after 1 day stirring or heating. After 1 h, the solvent was removed under vacuum and the residue extracted with hot toluene to afford a deep red solution. An abundant crop of red needles of **8** of good X-ray quality (0.41 g, 51% based on WCl_4) was obtained by slow diffusion of hexanes into the toluene solution at room temperature for 15 h. However, compound **8** was readily oxidized (or disproportionated) in solutions at room temperature to form a pink solution. We were able to identify one of the decomposition products to be $[WOCl(dppe)_2]^+$ on the basis of $^{31}P\{^1H\}$ NMR and UV−vis spectral data.[6]

IR data (cm^{-1}): 3061 (w), 3043 (w), 1495 (m), 1484 (m), 1433 (s), 1407 (w), 1356 (m), 1299 (vw), 1287 (vw), 1261 (m), 1186 (m), 1160 (w), 1149 (w), 1100 (s), 1090 (m), 1075 (w), 1064 (w), 1038 (w), 1027 (w), 1002 (m), 920 (vw), 879 (w), 862 (m), 835 (w), 800 (s), 750 (s), 744 (s), 740 (s), 735 (s), 705 (s), 693 (s), 677 (m), 668 (w).

^1H NMR data (C_6D_6, 24 °C, δ): 0.87 (t, $J = 7.0$ Hz, 6H, distal CH_3), 1.50 (t, $J = 7.0$ Hz, 6H, proximal CH_3), 2.33 (virtual t, $J = 9.8$ Hz, 2H, $P(CH_2)_2P$), 2.37 (m, 2H, distal NCH_2CH_3), 2.74 (m, 2H, distal NCH_2CH_3), 3.17 (virtual t, $J = 9.8$ Hz, 2H, $P(CH_2)_2P$), 4.78 (m, 2H, proximal NCH_2CH_3), 6.01 (m, 2H, proximal NCH_2CH_3), 6.75−7.36 (m, 20H, Ph).

$^{31}P\{^1H\}$ NMR data ($C_6D_6 + CH_2Cl_2$, 19 °C, δ): 9.47 (s, $^1J_{W-P} = 80$ Hz, $^3J_{P-P} = 12.8$ Hz).

FAB/DIP (NBA, neat, *m/z*): 1051 ($[M]^+$), 1016 ($[M - Cl]^+$), 980 ($[M - 2Cl]^+$ or $[M - NEt_2]^+$), 945 ($[M - 3Cl]^+$ or $[M - Cl - NEt_2]^+$).

Physical Measurements. The IR spectra were recorded on a Perkin-Elmer 16PC FT-IR spectrophotometer as Nujol mulls between KBr plates. ^1H NMR spectral measurements were performed on a Varian

(6) Chiu, K. W.; Lyons, D.; Wilkinson, G. *Polyhedron* **1983**, *2*, 803.

XL-200 spectrometer operating at 200 MHz. ^1H NMR chemical shifts are referenced to the residual proton impurity in the deuterated solvent. The $^{31}P\{^1H\}$ NMR data (81 MHz) were obtained at room temperature on a Varian XL-200 broad band spectrometer with the chemical shift values referenced externally and are reported relative to 85% H_3PO_4/D_2O. The FAB/DIP (DIP = direct insertion probe) mass spectra were acquired using a VG Analytical 70S high-resolution, double-focusing, sectored (EB) mass spectrometer. The instrument is equipped with a VG 11/250J data system that allowed computer control of the instrument, data recording, and data processing. Samples for analysis were prepared either by dissolving neat solid compound in *m*-nitrobenzyl alcohol (NBA) matrix or mixing a solution of the compound in CH_2Cl_2 or C_6H_6 with an NBA matrix on the direct insertion probe tip. The probe was then inserted into the instrument through a vacuum interlock and the sample bombarded with 8 keV xenon primary particles from an Ion Tech FAB gun operating at an emission current of 2 mA. Positive secondary ions were extracted and accelerated to 6 keV and then mass analyzed.

X-ray Crystallographic Procedures. Single crystals of compounds **1**−**8** were obtained as described in the Experimental Section. Geometric and intensity data were collected on the following diffractometers: Rigaku AFC7R (**1**), Rigaku AFC5R (**2** and **8**·C_7H_8), Enraf-Nonius CAD-4S (**5**·C_7H_8 and **6**·CH_2Cl_2), and Enraf-Nonius FAST (**3**, **4a,b**, **7**). Detailed procedures have previously been described.[1,2] For the crystals on the CAD-4S and Rigaku diffractometers, unit cells were determined by using search, center, index, and least-squares routines. The Laue classes and lattice dimensions were verified by axial oscillation photography. The intensity data were corrected for Lorentz and polarization effects and for decay where necessary. Empirical absorption corrections based on a series of Ψ scans were also applied.[7] For the crystals on the FAST diffractometer, a preliminary data collection was first carried out to afford all parameters and an orientation matrix. Fifty reflections were used in cell indexing and 250 reflections in cell refinement. Axial images were used to confirm the Laue group and cell dimensions. All calculations were performed on a DEC 3000-800 AXP workstation. The coordinates of W atoms for all structures were determined by direct methods as programmed in SHELXS-86[8] or SHELXTL.[9] The positions of the remaining non-hydrogen atoms were located using subsequent sets of least-squares refinement cycles followed by difference Fourier syntheses using the SHELXL-93 structure refinement program.[10] These positions were initially refined with isotropic displacement parameters and then with anisotropic displacement parameters to convergence. Except for compounds **1** and **6**·CH_2Cl_2, hydrogen atoms were included in the structure factor calculations at idealized positions in each model and were allowed to ride on the neighboring carbon atoms. Crystallographic data and refinement results for **1**−**8** are summarized in Table 1. Tables 2 and 4 list the selected bond distances and angles for the *cis,trans*- and *cis,cis*-isomers, respectively. Tables 3 and 5 tabulate the important torsional angles about the W−W axis for **1**−**7**. The important molecular parameters for **8** are presented in Table 6. Tables of positional and isotropic parameters, and anisotropic displacement parameters as well as complete tables of bond distances and angles and coordinates of hydrogen atoms are available as Supporting Information.

***cis,trans*-$W_2Cl_4(NEt_2)_2$(dmpm) (1).** A dark-red crystal with the approximate dimensions of 0.50 × 0.10 × 0.10 mm was mounted and sealed inside a Lindemann capillary. The unit cell constants were determined from 25 reflections in the range $12 < 2\theta < 17°$. Data collection was carried out with an $\omega-2\theta$ scan motion in the range $4 < 2\theta < 48°$. There was no observable decay during the data collection. Systematic absences narrowed the choice of space groups to *C*2/*c* and *Cc*. The centrosymmetric space group, *C*2/*c*, was selected for initial

Table 1. Crystallographic Data for *cis,trans*-$W_2Cl_4(NEt_2)_2$(dmpm) (**1**), *cis,cis*-$W_2Cl_4(NEt_2)_2$(dmpm) (**2**), *cis,trans*-$W_2Cl_4(NBu_2)_2$(dmpm) (**3**), *cis,cis*-$W_2Cl_4(NBu_2)_2$(dmpm) (**4a,b**), *cis,cis*-$W_2Cl_4(NHex_2)_2$(dmpm) (**5**), *cis,trans*-$W_2Cl_4(NEt_2)_2$(dmpe) (**6**), *cis,trans*-$W_2Cl_4(NBu_2)_2$(dmpe) (**7**), and *trans,trans*-$W_2Cl_4(NEt_2)_2$(dppe) (**8**)

	1	**2**	**3**	**4a**	**4b**	**5**·C_7H_8	**6**·CH_2Cl_2	**7**	**8**·C_7H_8
formula	$W_2Cl_4P_2C_{13}H_{34}N_2$	$W_2Cl_4P_2C_{13}H_{34}N_2$	$W_2Cl_4P_2C_{21}H_{50}N_2$	$W_2Cl_4P_2C_{21}H_{50}N_2$	$W_2Cl_4P_2C_{21}H_{50}N_2$	$W_2Cl_4P_2C_{36}H_{74}N_2$	$W_2Cl_6P_2C_{15}H_{38}N_2$	$W_2Cl_4P_2C_{22}H_{52}N_2$	$W_2Cl_4P_2C_{41}H_{52}N_2$
fw	789.86	789.86	902.07	902.07	902.07	1106.41	888.81	916.10	1144.29
space group	*C*2/*c* (No. 15)	$P2_1/c$ (No. 14)	*Pbca* (No. 61)	*C*2/*c* (No. 15)	*Pbca* (No. 61)	*C*2/*c* (No. 15)	$P2_1/c$ (No. 14)	$P2_1/n$ (No. 14)	$P2_1/n$ (No. 14)
a, Å	33.210(3)	8.760(3)	14.958(2)	18.011(4)	14.772(2)	18.368(4)	9.596(2)	9.465(1)	16.396(3)
b, Å	8.725(4)	21.028(8)	15.823(2)	17.221(4)	17.188(1)	17.060(2)	15.975(2)	34.545(7)	10.104(2)
c, Å	17.052(4)	12.778(5)	27.8014(9)	21.264(6)	25.370(3)	30.414(4)	18.756(4)	10.177(4)	26.680(2)
β, deg	100.44(1)	91.77(3)	90	103.33(2)	90	103.96(1)	96.73(1)	97.220(1)	92.22(2)
V, Å^3	4859(3)	2353(1)	6580(1)	6418(3)	6442(1)	9249(3)	2855.4(9)	3301(2)	4417(1)
Z	8	4	8	8	8	8	4	4	4
ρ_{calc}, g/cm^3	2.159	2.230	1.821	1.867	1.860	1.589	2.068	1.843	1.721
μ, mm^{-1}	10.033	23.269	7.422	7.609	7.581	5.296	8.731	7.398	12.624
radiation (*λ*, Å)	Mo Kα (0.710 73)	Cu Kα (1.541 84)	Mo Kα (0.710 73)	Mo Kα (0.710 73)	Mo Kα (0.710 73)	Mo Kα (0.710 73)	Mo Kα (0.710 73)	Mo Kα (0.710 73)	Cu Kα (1.541 84)
temp, °C	20	20	-60	-60	-60	-100	-100	-60	20
$R1$,[a] $wR2$[b] [$I > 2\sigma(I)$]	0.023, 0.046	0.059, 0.166	0.045, 0.108	0.061, 0.125	0.040, 0.086	0.047, 0.107	0.026, 0.065	0.047, 0.106	0.042, 0.108
$R1$,[a] $wR2$[b] (all data)	0.055, 0.058	0.063, 0.170	0.094, 0.139	0.133, 0.149	0.098, 0.114	0.107, 0.132	0.032, 0.071	0.075, 0.130	0.056, 0.117

[a] $R1 = \sum||F_o| - |F_c||/\sum|F_o|$. [b] $wR2 = [\sum[w(F_o^2 - F_c^2)^2]/\sum[w(F_o^2)^2]]^{1/2}$.

(7) (a) North, A. C. T.; Phillips, D. C.; Mathews, F. S. *Acta Crystallogr., Sect. A* **1968**, *A24*, 351. (b) TEXSAN: Crystal Structure Analysis Package, Molecular Structure Corp., Houston, TX, 1985 and 1992.
(8) Sheldrick, G. M. In *Crystallographic Computing 3*; Sheldrick, G. M., Kruger, C., Goddard, R., Eds.; Oxford University Press: Oxford, U.K., 1985; p 175.
(9) SHELXTL V. 5, Siemens Industrial Automation Inc., 1994.
(10) Sheldrick, G. M. In *Crystallographic Computing 6*; Flack, H. D., Parkanyi, L., Simon, K., Eds.; Oxford University Press: Oxford, U.K., 1993, p 111.

refinement, and this choice proved satisfactory. Hydrogen atoms were located from difference Fourier maps and were refined. The largest remaining peak in the final difference Fourier map was 0.74 e/Å^3.

***cis,cis*-$W_2Cl_4(NEt_2)_2$(dmpm) (2).** A red crystal with dimensions of 0.35 × 0.15 × 0.10 mm was mounted on the top of a glass fiber with epoxy cement. Centering, indexing, and a least-squares calculation on the 25 reflections with $58 < 2\theta < 78$ ° (Cu Kα radiation) gave a monoclinic crystal system. The intensity data were gathered by the $\omega-2\theta$ scan method in the range $8 < 2\theta < 120°$. No crystal decay was observed. The space group $P2_1/c$ was assigned from systematic absences. The largest peak in the difference Fourier map was 2.76 e/Å^3, lying 1.28 Å from W atom.

***cis,trans*-$W_2Cl_4(NBu_2)_2$(dmpm) (3).** A tiny red block of dimensions 0.18 × 0.13 × 0.13 mm was mounted with silicone grease on the tip of a quartz fiber and immediately placed in a stream of cold nitrogen at −60 °C. The intensity data were collected with an area detector for $4 < 2\theta < 50°$. The data were corrected for Lorentz and polarization effects by the MADNES program.[11] Systematic absences in the data uniquely determined the space group to be *Pbca*. The data were corrected for absorption anisotropy effects using a local adaptation of the program SORTAV.[12] All the non-hydrogen atoms were refined anisotropically. The final difference Fourier map showed no significant peaks other than those located in the vicinity of the W atoms.

***cis,cis*-$W_2Cl_4(NBu_2)_2$(dmpm) (4a,b).** Crystals of **4a,b** obtained by slow diffusion of hexanes into the CH_2Cl_2 solution were separated under a microscope on the basis of the different shapes of the crystals (red-brown blocks for **4a** and red needles for **4b**). For **4a**, a red-brown block-shaped crystal of dimensions 0.13 × 0.08 × 0.05 mm was selected and mounted on the end of a quartz fiber with grease. Data collection was carried out in the range $4 < 2\theta < 50°$. The space group *C*2/*c* was chosen and confirmed by successful solution and refinement of the structure. Direct methods led to the location of the positions of W(1) and W(2) of two crystallographically independent molecules. The rest of the structure was developed in a series of alternating difference Fourier maps and least-squares refinements. No absorption corrections were applied. Anisotropic displacement parameters were used for all the non-hydrogen atoms. The final difference map contained several small "ghost" peaks in close proximity to the heavy atoms, but no effort was made to correct for this problem.

For **4b**, a red needle with dimensions of 0.50 × 0.08 × 0.05 mm was mounted on the tip of a quartz fiber with grease and kept at −60 °C throughout the experiment. The intensity data were collected for $4 < 2\theta < 50°$. Systematic absences in the data led to the space group *Pbca*. Direct methods revealed the location of two W atoms of a dinuclear unit. The use of alternating difference Fourier maps and least-squares refinements gave the positions of all the remaining non-hydrogen atoms. The program SORTAV was used to correct for absorption. All non-hydrogen atoms were refined anisotropically. The final difference map was essentially featureless, the largest peaks being associated with the W atoms.

***cis,cis*-$W_2Cl_4(NHex_2)_2$(dmpm) (5).** A red block-shaped crystal with dimensions of 0.35 × 0.23 × 0.18 mm was selected and fixed on the tip of a quartz fiber with grease at −100 °C in the diffractometer. Indexing based on 24 reflections resulted in a monoclinic cell and the cell parameters were further refined in the range $27 < 2\theta < 31°$. The intensity data were gathered by the $\omega-\theta$ scan technique for $4 < 2\theta < 46°$. No significant decay was found during the data collection. After isotropic refinement of all atoms of the dinuclear complex, the difference Fourier map showed several peaks that could be ascribed to solvent molecules. These peaks were modeled as toluene molecules, and there were eight C_7H_8 molecules per unit cell. After the heavy atoms had been refined anisotropically, it became apparent that all four hexyl chains of both independent molecules were disordered. This disorder was modeled by constraining the displacement parameters to be equal and restraining the chemically equivalent bonds to be approximately equal. Also, the site occupany factors were allowed to vary but were constrained so that the sum equaled to 1. The resulting model yielded reasonable bond distances and angles. All the nondisordered non-hydrogen atoms were then refined anisotropically. The final difference electron density map had no significant features other than several small peaks close to W atoms.

***cis,trans*-$W_2Cl_4(NEt_2)_2$(dmpe) (6).** A red block-shaped crystal having dimensions of 0.50 × 0.35 × 0.28 mm was mounted on the top of a quartz fiber with grease. A monoclinic cell was obtained based on the 25 reflections with 2θ values 36−40°. The intensities of all reflections with 2θ values in the range 4−54° were measured by the $\omega-\theta$ scan technique. The space group $P2_1/c$ was identified uniquely from the systematic absences in the data. After all the non-hydrogen atoms of the whole dinuclear complex had been located, the difference Fourier map still had three significant peaks which appeared to be a CH_2Cl_2 solvent molecule. The non-hydrogen atoms in both molecules were refined anisotropically. Hydrogen atoms were then included and refined. This model was refined to convergence and the final difference electron density map revealed only one peak above 1 e/Å^3, lying 1.10 Å from W(1).

***cis,trans*-$W_2Cl_4(NBu_2)_2$(dmpe) (7).** An orange-red crystal of dimensions 0.30 × 0.15 × 0.10 mm was carefully selected and mounted on the top of a quartz fiber. The intensity data were measured in the range $4 < 2\theta < 43°$. The space group $P2_1/n$ was determined based on the systematic absences. Absorption corrections based on the SORTAV program were applied. The largest remaining peak in the final difference map was 0.83 e/Å^3, located 1.25 Å from W atom.

***trans,trans*-$W_2Cl_4(NEt_2)_2$(dppe) (8).** A red needle-shaped crystal with dimensions of 0.80 × 0.10 × 0.10 mm was glued on the tip of a glass fiber with epoxy cement. Compound **8** crystallized in the monoclinic crystal system based on the 25 reflections with 2θ ranging from 28 to 35° (Cu Kα radiation). An $\omega-2\theta$ scan method was used to collect the intensity data for $6 < 2\theta < 115°$. A significant decay in intensity was observed during the entire period of data collection, and an appropriate decay correction was applied. Systematic absences uniquely determined the space group as $P2_1/n$. The difference Fourier map showed several peaks that could be assigned to be solvent molecules. These peaks were modeled as toluene molecules. In each C_7H_8 molecule, all carbon atoms were found to be disordered over two sites. All the non-hydrogen atoms, except the carbon atoms for the toluene solvent molecule, were refined with anisotropic displacement parameters. A final difference Fourier map revealed that the highest remaining peak of electron density (0.72 e/Å^3) was located near W(1).

Results and Discussion

Synthesis, Solubility and Stability. The preparation of triply-bonded complexes $W_2Cl_4(NR_2)_2$(L-L) (R = Et, L-L = dmpm, dmpe, dppe; R = Bu, L-L = dmpm, dmpe; R = Hex, L-L = dmpm) proceeds straightforwardly via reaction of $W_2Cl_4(NR_2)_2(NHR_2)_2$ (R = Et, Bu, Hex) with 1 equiv of the appropriate bidentate phosphines at room temperature. Reactions involving dmpm or dmpe readily afford products in three isomeric forms, *trans,trans*-, *cis,trans*-, and *cis,cis*-$W_2Cl_4(NR_2)_2$(L-L) (R = Et, Bu, Hex; L-L = dmpm, dmpe) with proportions depending on the reaction time as well as the diphosphines and dialkylamido groups used (Scheme 1). When $W_2Cl_4(NR_2)_2(NHR_2)_2$ (R = Et, Bu, Hex) and dmpm are allowed to react in tetrahydrofuran or toluene, the major products are *trans,trans*-$W_2Cl_4(NR_2)_2$(dmpm) (R = Et, Bu, Hex) initially. However, attempts to isolate this type of isomer are not yet successful. According to $^{31}P\{^1H\}$ NMR spectroscopic studies of the reaction mixture, the concentration of the *trans,trans*-isomer in each case gradually decreased with time while the amount of the other two isomers continuously built up. In each case, all the *trans,trans*-isomer eventually disappeared, and thus, the failure, so far, to isolate the pure *trans,trans*-isomer can be understood. When the mixture was allowed to stand at room temperature, only the *cis,cis*-isomer, as identified by $^{31}P\{^1H\}$ NMR spectroscopy, remained at the end. We believe that the *trans,trans*-isomer of the type $W_2Cl_4(NR_2)_2$(dmpm) (R = Et, Bu, Hex) is

(11) Pflugrath, J.; Messerschmitt, A. MADNES, Munich Area Detector (New EEC) System, version EEC 11/9/89, with enhancements by Enraf-Nonius Corp., Delft, The Netherlands. A description of MADNES appears in: Messerschmitt, A.; Pflugrath, J. *J. Appl. Crystallogr.* **1987**, *20*, 306.

(12) Blessing, R. H.; *Acta Crystallogr., Sect. A* **1995**, *A51*, 33.

Scheme 1

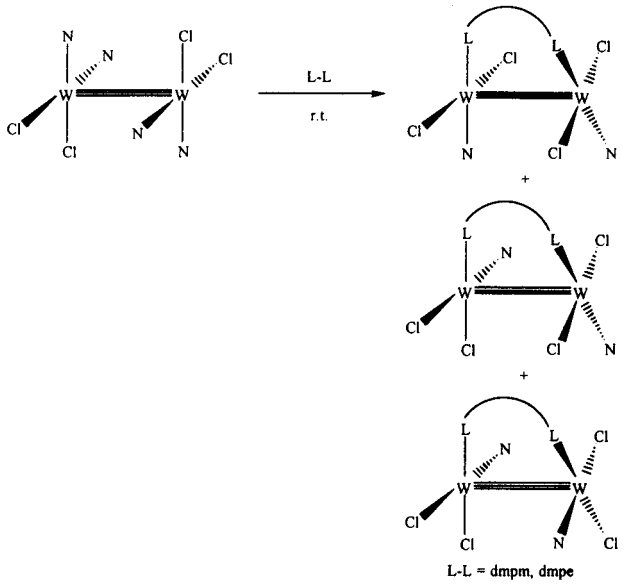

the kinetic product. The *trans,trans*-isomer slowly isomerizes in solution to form first the *cis,trans*-isomer and finally the thermodynamically favored *cis,cis*-isomer. Moreover, a sample of *cis,cis*-isomer was left in CH_2Cl_2 for 1 week and showed no indication of isomerization back to either *cis,trans*- or *trans, trans*-isomer. In the case of dmpe, the *trans,trans*-isomers again seem to be the kinetically favored products in each case. However, they are much more thermodynamically stable than their dmpm counterparts and can be easily isolated by extracting the products into hexanes. On the other hand, the reaction of $W_2Cl_4(NEt_2)_2(NHEt_2)_2$ with another diphosphine ligand having two carbon atoms linking the phosphorus atoms, namely, dppe, forms purely the *trans,trans*-isomer **8** in 51% yield. When a pure sample of **8** in solution was monitored by $^{31}P\{^1H\}$ NMR spectroscopy at room temperature, no evidence of isomerization to any other isomers was observed which, at first sight, means that the isomerization barrier might be too high for interconversion at ambient temperature (i.e. kinetically stabilized). Attempts were then made to heat the sample solution up to 80 °C, but the spectrum remained more or less the same. Hence, compound **8** is both the kinetically and thermodynamically favored isomer in this case.

The *trans,trans*-isomers of $W_2Cl_4(NR_2)_2(dmpe)$ (R = Et, Bu) are very soluble in hexanes. The rest of the compounds exhibit fair solubility in toluene and benzene and higher solubility in CH_2Cl_2. All the compounds appear to be air stable for short periods of time in the solid state. In solution, they slowly decompose upon exposure to air. This was evidenced by the observation of a significant amount of $[WOCl(dppe)_2]^+$ in the $^{31}P\{^1H\}$ NMR spectrum of **8**.

Spectroscopic Properties. All complexes of $W_2Cl_4(NR_2)_2(L\text{-}L)$ reported here exhibit parent molecular ion peaks M^+ in their mass spectra, and many W_2-containing fragment ions were observed. Losses of chlorine ligands and amido groups are competitive processes during fragmentation. For all the compounds except **6** and **7**, the most abundant fragment ion is $[W_2Cl_4(NR_2)(L\text{-}L)]^+$ in each case. In contrast, the fragment ions $[W_2Cl_3(NR_2)_2(dmpe)]^+$ (R = Et, Bu) appear as the most intense peaks in the mass spectra of **6** and **7**. It is interesting to note that fission of the metal−metal bond is not facile for this kind of complex under the experimental conditions.

The ^1H NMR spectra of all the available compounds clearly show that substitution of both dialkylamino groups by the appropriate bidentate phosphines took place. At room temperature, compounds **2**, **6**, and **8** display well-separated proximal and distal NEt resonances akin to those reported for $W_2Cl_4(NR_2)_2(PR'_3)_2$ molecules.[2] It is noteworthy that, for **6** with a *cis,trans*-stereochemistry, each set of proximal and distal NEt signals is further split into another set due to the different chemical environment caused by the phosphorus atoms *cis* and *trans* to the NEt_2 groups. This makes the interpretation of the corresponding spectrum more difficult. For those compounds with NBu_2 and $NHex_2$ groups, proximal and distal resonances were also observed for the CH_2CH_3 groups. The spectra were, however, complicated by the signals arising from diphosphine ligands and other methylene protons. Because of the low stability of **1** and **3** in all common organic solvents, it was impossible to obtain decent NMR spectra of these two compounds.

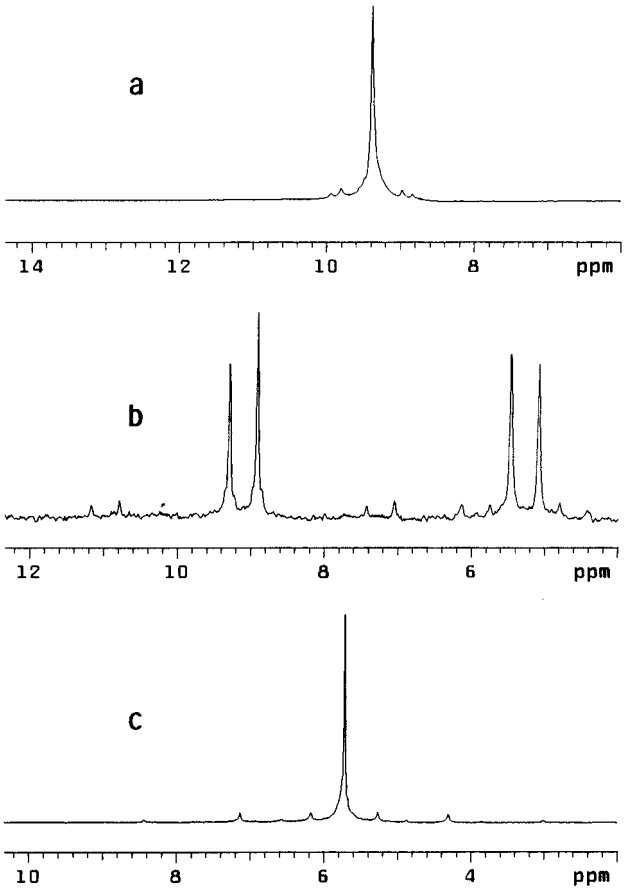

Figure 2. $^{31}P\{^1H\}$ NMR spectra of (a) *trans,trans*-$W_2Cl_4(NEt_2)_2(dppe)$ in C_6D_6/CH_2Cl_2, (b) *cis,trans*-$W_2Cl_4(NEt_2)_2(dmpe)$ in C_6D_6 and (c) *cis,cis*-$W_2Cl_4(NHex_2)_2(dmpm)$ in C_6D_6, at room temperature.

The identities of the three isomeric types of dinuclear complex observed in this study are readily established by their distinctive $^{31}P\{^1H\}$ NMR spectra. Figure 2a−c provides representative $^{31}P\{^1H\}$ NMR spectra for each of the isomers studied. As expected for ABX ($PP^{183}W$) systems in *cis*- and *trans*-$W_2Cl_4(NHCMe_3)_2(PR_3)_2$ molecules,[13] both *cis,cis*- and *trans, trans*-isomers consist of strong central singlets flanked by weak satellites due to $^{31}P-^{183}W$ coupling. In each case, approximate P-P coupling constants may be deduced from the satellite doublets. The spectra of *cis,trans*-$W_2Cl_4(NR_2)_2(L\text{-}L)$ molecules are of particular interest as they provide a unique opportunity to examine the characteristics of diphosphines on dinuclear complexes in such an unprecedented bonding mode. The full

(13) Chen, H.; Cotton, F. A.; Yao, Z. *Inorg. Chem.* **1994**, *33*, 4255.

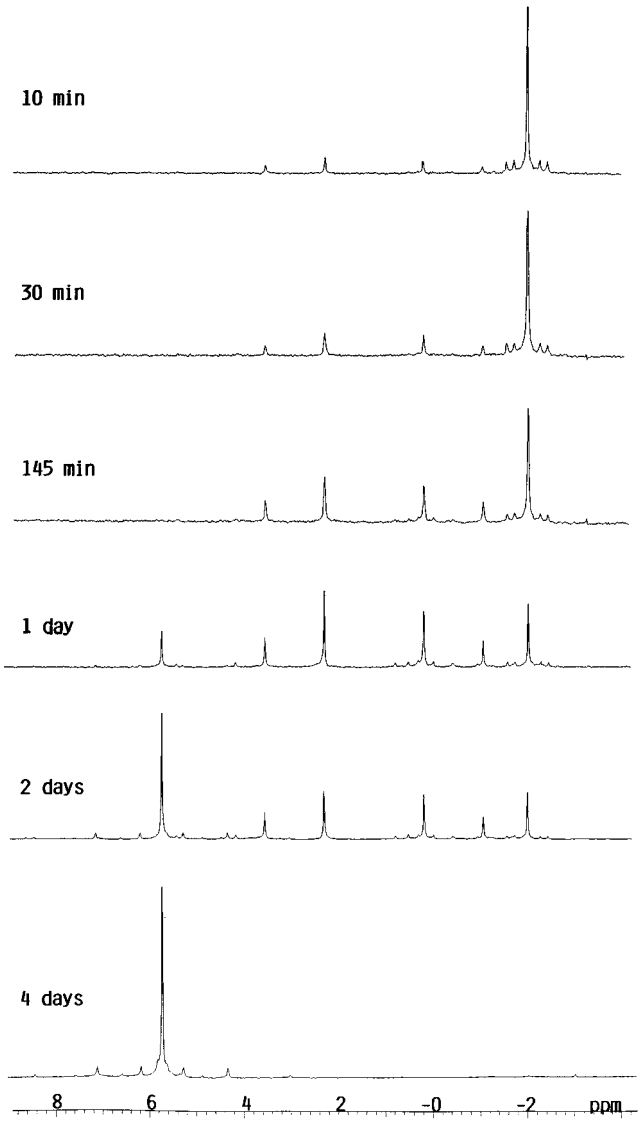

Figure 3. $^{31}P\{^1H\}$ NMR spectra of $W_2Cl_4(NHex_2)_2$(dmpm) at various time intervals in C_6D_6/THF, showing the interconversion among the three distinct isomers at room temperature.

proton-decoupled ^{31}P NMR spectrum of **6**, shown in Figure 2b, consists of a set of two intense doublets centered at 5.58 and 8.92 ppm. The upfield and downfield resonances are tentatively assigned to the phosphorus atom cis and trans to NBu_2 groups, respectively. The assignments were made on the basis of $^{31}P-^{183}W$ coupling observed in the spectrum. A notable feature in this spectrum is the prominence of the set of ^{183}W satellites and its complexity, relative to those of the *cis,cis*- and *trans,trans*-isomers. The magnitude of the $^1J_{W-P}$(cis) coupling (292 Hz) is significantly larger than that for the trans phosphorus atom (141 Hz), as one might expect.[13] It can be seen clearly that the four intense signals in Figure 2b do not have equal intensities, the so-called "roof effect". To obtain such a coupling scheme, it is necessary to consider an AB system when ^{183}W coupling is ignored. As defined in Figure 2b, the chemical shifts for each P atom are given by $\nu_{cis} = \nu_z + \Delta\nu/2$ and $\nu_{trans} = \nu_z - \Delta\nu/2$, where $\Delta\nu = (|(f_1 - f_4)(f_2 - f_3)|)^{1/2}$ Hz and f_1, f_2, f_3, and f_4 are the resonance frequencies of the four lines of the AB spectrum.[14] Such an AB system thus gives rise to the observed doublet of doublets with ν_{cis} at 8.92 ppm, ν_{trans} at 5.58 ppm and $^3J_{P-P} = 32.5$ Hz. However, due to the poor quality of the low-intensity portion of the spectrum, the values of the coupling

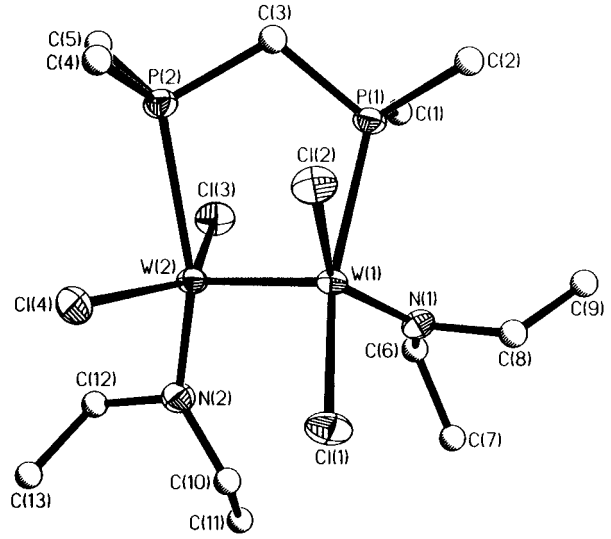

Figure 4. Perspective drawing of *cis,trans*-$W_2Cl_4(NEt_2)_2$(dmpm) (**1**). Atoms are represented by thermal ellipsoids at the 40% probability level. Carbon atoms are shown as spheres of arbitrary radii.

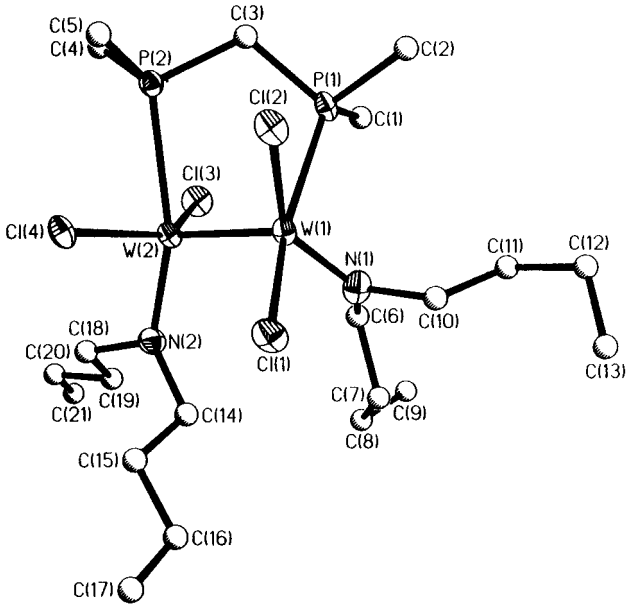

Figure 5. Perspective drawing of *cis,trans*-$W_2Cl_4(NBu_2)_2$(dmpm) (**3**). Atoms are represented by thermal ellipsoids at the 40% probability level. Carbon atoms are shown as spheres of arbitrary radii.

constants determined should only be regarded as approximate. Also, a noteworthy feature is that the J_{W-P} and J_{P-P} values for each particular type of isomer are relatively insensitive to the variation of the amido ligands for a given diphosphine used.

As mentioned in the foregoing section, preliminary results indicate that the relative concentrations of the three isomers of $W_2Cl_4(NR_2)_2$(dmpm) in solution are dependent on the reaction time. The results of a run for $W_2Cl_4(NHex_2)_2$(dmpm) in which the *trans,trans*-compound was converted to a *cis,trans*/*cis,cis*-mixture in C_6D_6/THF at room temperature at various times are shown in Figure 3. It can be seen that the conversion was completed in 4 days, leaving only the *cis,cis*-isomer in the mixture. Although the exact mechanism for this isomerization is obscure, the reaction is completely reproducible.

Structure and Bonding. The $W_2Cl_4(NR_2)_2$(L-L) compounds **1**−**8** reported here have been characterized by X-ray crystal-

(14) Friebolin, H. *Basic One- and Two-Dimensional NMR Spectroscopy*, 2nd ed.; VCH: New York, 1993.

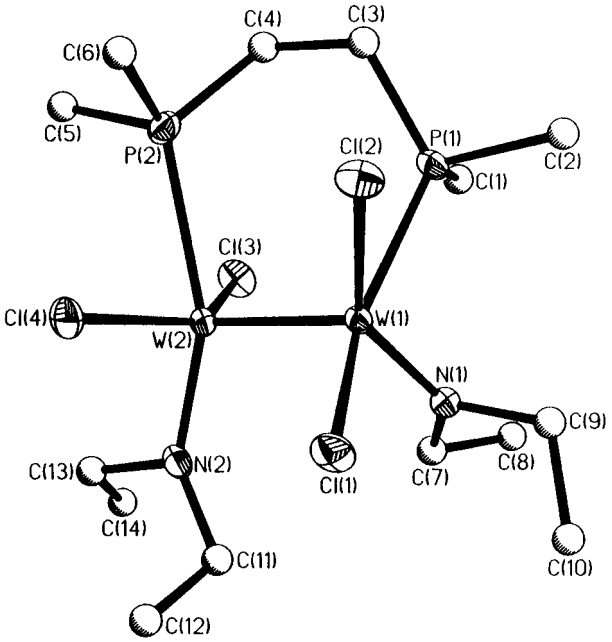

Figure 6. Perspective drawing of *cis*,*trans*-$W_2Cl_4(NEt_2)_2$(dmpe) (**6**). Atoms are represented by thermal ellipsoids at the 40% probability level. Carbon atoms are shown as spheres of arbitrary radii.

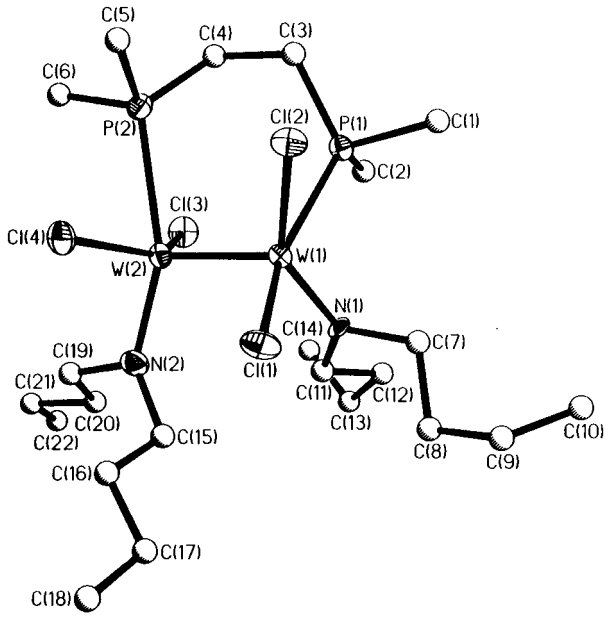

Figure 7. Perspective drawing of *cis*,*trans*-$W_2Cl_4(NBu_2)_2$(dmpe) (**7**). Atoms are represented by thermal ellipsoids at the 40% probability level. Carbon atoms are shown as spheres of arbitrary radii.

lography. The molecules possess a common W_2^{6+} unit having eight ligated atoms and geometries based on a $W_2Cl_4P_2N_2$ core. Each W atom in the molecule is approximately square planar with two Cl, one P, and one N atoms coordinated to it. The two pseudoplanar WCl_2PN units united by a W−W triple bond are staggered with respect to each other and the central $(W{\equiv}W)^{6+}$ unit is spanned by a bridging diphosphine. An interesting difference between various isomeric compounds lies in the way the two phosphorus atoms of the diphosphine are bonded to the W atoms with respect to the amido groups. In no case was any disorder problem of the W_2 units in the crystals encountered. The W−W bond distances span the narrow range of 2.314−2.341 Å and fall within the range of the bond distances established for the W≡W bond with a $\sigma^2\pi^4$ ground-state electronic configuration.[15] Comparison between $W_2Cl_4(NR_2)_2(PR'_3)_2$[2] and $W_2Cl_4(NR_2)_2$(L-L) (L-L = bidentate phosphines)

Table 2. Selected Bond Distances (Å) and Angles (deg) for *cis*,*trans*-$W_2Cl_4(NEt_2)_2$(dmpm) (**1**), *cis*,*trans*-$W_2Cl_4(NBu_2)_2$(dmpm) (**3**), *cis*,*trans*-$W_2Cl_4(NEt_2)_2$(dmpe) (**6**), and *cis*,*trans*-$W_2Cl_4(NBu_2)_2$-(dmpe) (**7**)

	1	**3**	**6**	**7**
W(1)−W(2)	2.3259(5)	2.3261(6)	2.3136(4)	2.3182(8)
W(1)−P(1)	2.510(2)	2.522(3)	2.518(1)	2.525(3)
W(2)−P(2)	2.654(2)	2.611(3)	2.588(1)	2.596(4)
W(1)−N(1)	1.905(6)	1.90(1)	1.916(4)	1.910(9)
W(2)−N(2)	1.915(7)	1.929(9)	1.936(4)	1.95(1)
W(1)−Cl(1)	2.397(2)	2.399(3)	2.387(1)	2.391(3)
W(2)−Cl(4)	2.360(2)	2.365(3)	2.370(1)	2.362(3)
W(1)−Cl(2)	2.437(2)	2.427(3)	2.433(1)	2.440(3)
W(2)−Cl(3)	2.375(2)	2.368(3)	2.369(1)	2.374(3)
P(1)−W(1)−N(1)	88.3(2)	89.9(3)	88.4(1)	89.0(3)
P(1)−W(1)−Cl(1)	159.11(8)	158.4(1)	155.57(4)	155.0(1)
P(1)−W(1)−Cl(2)	77.83(8)	77.7(1)	77.73(4)	77.3(1)
N(1)−W(1)−Cl(1)	97.0(2)	96.6(3)	97.5(1)	96.7(3)
N(1)−W(1)−Cl(2)	143.1(2)	143.7(3)	143.4(1)	144.6(3)
Cl(1)−W(1)−Cl(2)	86.02(8)	85.1(1)	83.62(4)	84.2(1)
W(2)−W(1)−P(1)	92.67(5)	92.11(7)	97.49(3)	97.83(8)
W(2)−W(1)−N(1)	106.6(2)	104.7(3)	103.8(1)	103.2(3)
W(2)−W(1)−Cl(1)	105.00(6)	106.0(8)	103.99(3)	104.48(9)
W(2)−W(1)−Cl(2)	108.05(6)	109.62(7)	111.41(3)	110.77(8)
P(2)−W(2)−N(2)	161.9(2)	161.8(3)	156.8(1)	157.1(3)
P(2)−W(2)−Cl(3)	80.26(8)	79.5(1)	79.59(4)	78.6(1)
P(2)−W(2)−Cl(4)	81.71(8)	81.5(1)	79.24(4)	79.3(1)
N(2)−W(2)−Cl(3)	94.1(2)	95.5(3)	95.7(1)	95.8(3)
N(2)−W(2)−Cl(4)	93.4(2)	92.4(3)	92.5(1)	93.1(3)
Cl(3)−W(2)−Cl(4)	143.76(8)	141.8(1)	144.01(5)	142.8(1)
W(1)−W(2)−P(2)	91.74(5)	92.12(6)	97.63(3)	97.97(8)
W(1)−W(2)−N(2)	106.3(2)	105.9(3)	105.3(1)	104.8(3)
W(1)−W(2)−Cl(3)	110.66(6)	110.84(8)	109.97(3)	109.79(8)
W(1)−W(2)−Cl(4)	101.04(6)	102.67(7)	101.45(4)	102.62(9)

Table 3. Selected Torsion Angles (deg) for *cis*,*trans*-$W_2Cl_4(NEt_2)_2$(dmpm) (**1**), *cis*,*trans*-$W_2Cl_4(NBu_2)_2$(dmpm) (**3**), *cis*,*trans*-$W_2Cl_4(NEt_2)_2$(dmpe) (**6**), and *cis*,*trans*-$W_2Cl_4(NBu_2)_2$(dmpe) (**7**)

	1	**3**	**6**	**7**
P(1)−W(1)−W(2)−P(2)	-37.67(7)	-38.3(1)	-43.71(4)	-43.2(1)
P(1)−W(1)−W(2)−Cl(3)	42.57(8)	41.3(1)	37.94(4)	37.4(1)
N(1)−W(1)−W(2)−N(2)	54.4(3)	53.3(4)	49.8(2)	48.5(4)
N(1)−W(1)−W(2)−Cl(3)	-46.5(2)	-49.1(3)	-52.3(1)	-53.4(3)
Cl(1)−W(1)−W(2)−N(2)	-47.8(2)	-48.2(3)	-51.7(1)	-52.1(3)
Cl(1)−W(1)−W(2)−Cl(4)	49.18(8)	48.1(1)	44.04(5)	44.6(1)
Cl(2)−W(1)−W(2)−P(2)	40.40(8)	39.4(1)	36.00(4)	36.1(1)
Cl(2)−W(1)−W(2)−Cl(4)	-41.50(8)	-42.4(1)	-44.50(4)	-44.6(1)

molecules indicated that the bridging ligands do not cause any special shortness on the observed metal−metal bond lengths in these d^3−d^3 dinuclear compounds. The mean value of W−N distances (1.92 Å) in all molecules is within the range anticipated for such bonds. The specific characteristics of each complex and the relationships between them will be explored in the following paragraphs.

Compounds 1, 3, 6·CH_2Cl_2, and 7. Crystals of compounds **1** and **3** conform to the monoclinic space group *C*2/*c* and orthorhombic space group *Pbca*, respectively, with eight molecules per unit cell for each complex. Compounds **6** and **7** crystallize in the monoclinic space groups $P2_1/c$ and $P2_1/n$, respectively, with four molecules per unit cell. The structure of **6** contains a molecule of CH_2Cl_2. Perspective views of the structures of **1**, **3**, **6** and **7** are depicted in Figures 4−7. The core structures of all the compounds are very similar, and each molecule is chiral. The ligand arrangement found in these complexes belongs to the type II isomer (Figure 1) and has not previously been reported for other triply-bonded dinuclear complexes. It provides the first examples of a $W_2Cl_4P_2N_2$ type molecule in which one WCl_2PN unit has a cis arrangement while the other WCl_2PN unit has a trans arrangement. Hence, the two phosphorus atoms are non-equivalent in the molecule. In

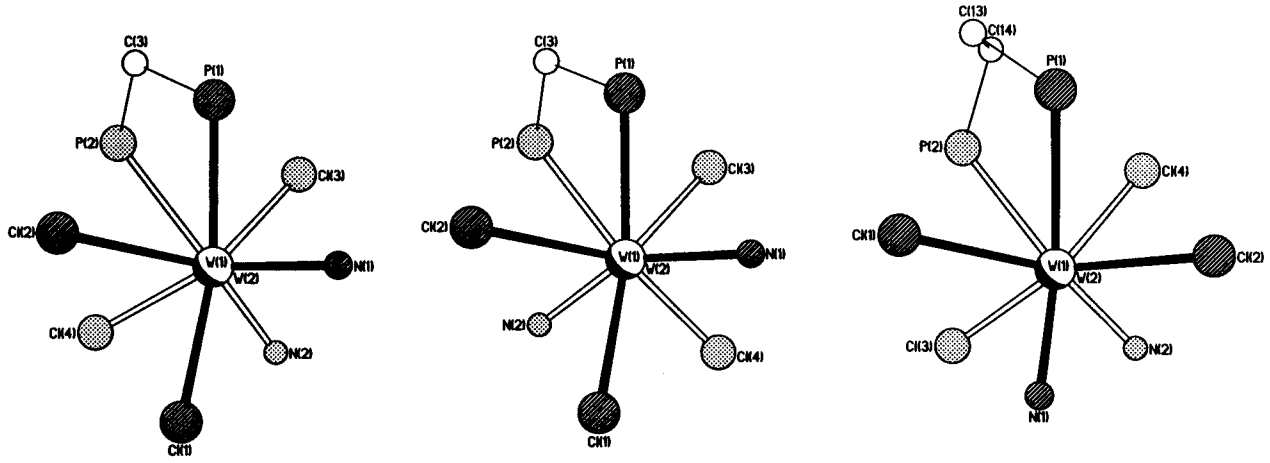

Figure 8. Views of the central part of (a, left) *cis,trans*-$W_2Cl_4(NEt_2)_2$(dmpm) (**1**), (b, center) *cis,cis*-$W_2Cl_4(NEt_2)_2$(dmpm) (**2**), and (c, right) *trans,trans*-$W_2Cl_4(NEt_2)_2$(dppe) (**8**) directly down W−W axis. Ethyl groups, methyl groups, and phenyl rings are omitted for clarity.

Table 4. Selected Bond Distances (Å) and Angles (deg) for *cis,cis*-$W_2Cl_4(NEt_2)_2$(dmpm) (**2**), *cis,cis*-$W_2Cl_4(NBu_2)_2$(dmpm) (**4a,b**) and *cis,cis*-$W_2Cl_4(NHex_2)_2$(dmpm) (**5**)

	2	**4a**[a]	**4b**	**5**[a]
W(1)−W(2)	2.332(1)	2.341(1)	2.3396(6)	2.340(1)
W(1)−P(1)	2.506(3)	2.515(5)	2.512(2)	2.519(3)
W(2)−P(2)	2.526(3)		2.529(3)	
W(1)−N(1)	1.918(9)	1.93(2)	1.918(8)	1.91(1)
W(2)−N(2)	1.92(1)		1.904(9)	
W(1)−Cl(1)	2.375(4)	2.406(4)	2.406(3)	2.399(3)
W(2)−Cl(4)	2.391(3)		2.407(3)	
W(1)−Cl(2)	2.432(3)	2.411(5)	2.421(3)	2.414(3)
W(2)−Cl(3)	2.417(3)		2.412(3)	
P(1)−W(1)−N(1)	87.3(3)	90.3(4)	88.4(2)	88.3(3)
P(1)−W(1)−Cl(1)	158.9(1)	159.7(2)	159.3(1)	161.4(1)
P(1)−W(1)−Cl(2)	77.7(1)	79.2(2)	79.34(9)	79.6(1)
N(1)−W(1)−Cl(1)	97.5(3)	92.8(4)	94.5(2)	95.0(3)
N(1)−W(1)−Cl(2)	142.9(3)	143.9(4)	143.4(3)	142.5(3)
Cl(1)−W(1)−Cl(2)	86.4(1)	86.7(2)	86.4(1)	87.0(1)
W(2)−W(1)−P(1)	93.15(8)	92.5(1)	92.23(7)	92.25(8)
W(2)−W(1)−N(1)	104.7(3)	104.4(4)	103.7(2)	103.7(3)
W(2)−W(1)−Cl(1)	105.4(1)	106.3(1)	106.91(7)	104.67(8)
W(2)−W(1)−Cl(2)	109.75(9)	110.5(1)	111.04(7)	112.05(9)
P(2)−W(2)−N(2)	89.8(3)		89.0(2)	
P(2)−W(2)−Cl(3)	80.4(1)		79.88(9)	
P(2)−W(2)−Cl(4)	162.0(1)		161.8(1)	
N(2)−W(2)−Cl(3)	142.4(3)		143.2(3)	
N(2)−W(2)−Cl(4)	93.9(3)		94.2(2)	
Cl(3)−W(2)−Cl(4)	86.0(1)		87.0(1)	
W(1)−W(2)−P(2)	91.41(8)		92.29(7)	
W(1)−W(2)−N(2)	103.6(3)		104.5(3)	
W(1)−W(2)−Cl(3)	112.75(9)		110.81(7)	
W(1)−W(2)−Cl(4)	104.8(1)		104.21(7)	

[a] Distances and angles are the averages for the two independent molecules of the asymmetric unit.

each case, it is clear that the W(1)−Cl(1) distance is shorter than the W(1)−Cl(2) distance (average Δ(W−Cl) = 0.04 Å) (Table 2). This is, no doubt, a manifestation of the trans influence which has been observed in many other systems[16] including $W_2Cl_4(NHCMe_3)_2$(L-L) (L-L = diphosphines)[1] and $W_2Cl_4(NR_2)_2(PR'_3)_2$.[2] On the other hand, the W(2)−Cl(3) and W(2)−Cl(4) distances are comparable to each other. One notable feature is an increase in the W(2)−P(2) distance relative to that observed in the *cis,cis*-counterparts (*vide infra*), and the

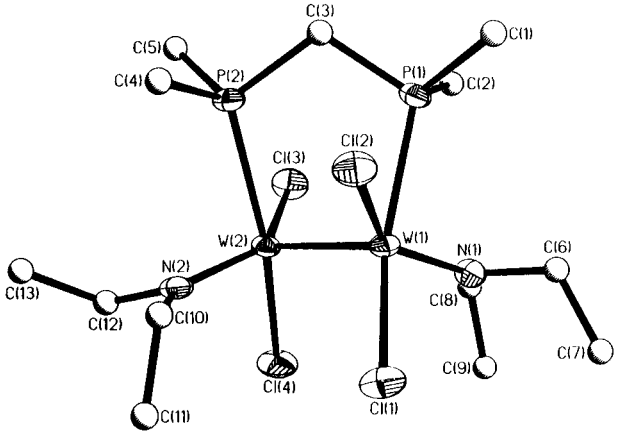

Figure 9. Perspective drawing of *cis,cis*-$W_2Cl_4(NEt_2)_2$(dmpm) (**2**). Atoms are represented by thermal ellipsoids at the 40% probability level. Carbon atoms are shown as spheres of arbitrary radii.

difference between W(1)−P(1) and W(2)−P(2) distances in these four molecules ranges from 0.07 to 0.14 Å (Table 2). This lengthening of the W−P bond distances is primarily attributed to the stronger trans influence of NR_2 groups compared to phosphine and chlorine ligands. Another striking structural feature of these molecules is the twisted configuration. Figure 8a shows a view of the inner part of a molecule of **1** looking down the W−W bond. This molecule displays a twisted configuration for the central portion with the torsional angle P(1)−W(1)−W(2)−P(2) being 37.7° (Table 3). The corresponding torsional angles for **3**, **6**, and **7** are 38.3, 43.7, and 43.2°, respectively.

Compounds 2, 4a, 4b, and 5·C_7H_8. Compound **2** crystallizes in the space group $P2_1/c$ with four molecules per unit cell. Compounds **4a** and **5** both conform to the space group $C2/c$ with two independent molecules in the asymmetric unit each. W(1) and W(1A) atoms form one dinuclear unit, and W(2) and W(2A) atoms form the other molecule. In total, there are eight $W_2Cl_4(NR_2)_2$(dmpm) molecules in the unit cell in each case. The crystals of **5** contain eight toluene solvent molecules in the unit cell. Compound **4b**, a polymorph of **4a**, crystallizes in the orthorhombic space group *Pbca* with eight W(1)−W(2) dinuclear units per unit cell. The molecular structures of **2**, **4a**, and **5** are shown in Figures 9−11, respectively.

The core structure of each molecule has only C_2 symmetry, and each molecule is chiral. In each case, the central $W_2Cl_4P_2N_2$ core unit has essentially the same structure with the two chlorine atoms in a cis position in each WCl_2PN unit and it is similar to

(15) Cotton, F. A.; Walton, R. A. *Multiple Bonds between Metal Atoms*, 2nd ed.; Oxford University Press: New York, 1993; see also references therein.

(16) (a) Cotton, F. A.; Felthouse, T. R. *Inorg. Chem.* **1981**, *20*, 3880. (b) Cotton, F. A.; Extine, M. W.; Felthouse, T. R.; Kolthammer, B. W. S.; Lay, D. G. *J. Am. Chem. Soc.* **1981**, *103*, 4040.

Table 5. Selected Torsion Angles (deg) for *cis,cis*-$W_2Cl_4(NEt_2)_2$(dmpm) (**2**), *cis,cis*-$W_2Cl_4(NBu_2)_2$(dmpm) (**4a,b**), and *cis,cis*-$W_2Cl_4(NHex_2)_2$(dmpm) (**5**)

	2	**4b**		**4a**[a]	**5**[a]
P(1)−W(1)−W(2)−P(2)	-36.9(1)	-37.33(9)	P(1)−W(1)−W(1A)−P(1A)	-36.3(2)	-37.3(2)
P(1)−W(1)−W(2)−Cl(3)	43.2(1)	42.7(1)	P(1)−W(1)−W(1A)−Cl(2A)	43.1(2)	42.4(1)
N(1)−W(1)−W(2)−Cl(3)	-44.8(3)	-46.2(2)	N(1)−W(1)−W(1A)−Cl(2A)	-47.8(5)	-46.3(3)
N(1)−W(1)−W(2)−Cl(4)	47.0(3)	46.0(2)	N(1)−W(1)−W(1A)−Cl(1A)	44.7(5)	46.3(3)
Cl(1)−W(1)−W(2)−N(2)	42.6(3)	45.2(3)	Cl(1)−W(1)−W(1A)−N(1A)	44.7(5)	46.3(3)
Cl(1)−W(1)−W(2)−Cl(4)	-55.2(1)	-53.1(1)	Cl(1)−W(1)−W(1A)−Cl(1A)	-52.6(2)	-52.7(2)
Cl(2)−W(1)−W(2)−P(2)	41.1(1)	42.1(1)	Cl(2)−W(1)−W(1A)−P(1A)	43.1(2)	42.4(1)
Cl(2)−W(1)−W(2)−N(2)	-49.0(3)	-47.4(3)	Cl(2)−W(1)−W(1A)−N(1A)	-47.8(5)	-46.3(3)

[a] Torsion angles are the averages for the two independent molecules of the asymmetric unit.

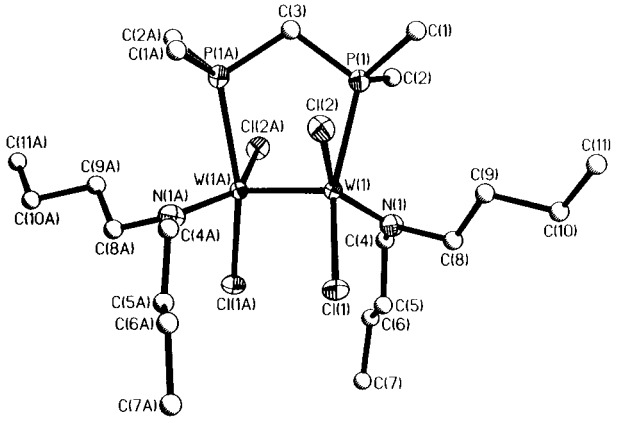

Figure 10. Perspective drawing of *cis,cis*-$W_2Cl_4(NBu_2)_2$(dmpm) (**4a**). Atoms are represented by thermal ellipsoids at the 40% probability level. Carbon atoms are shown as spheres of arbitrary radii.

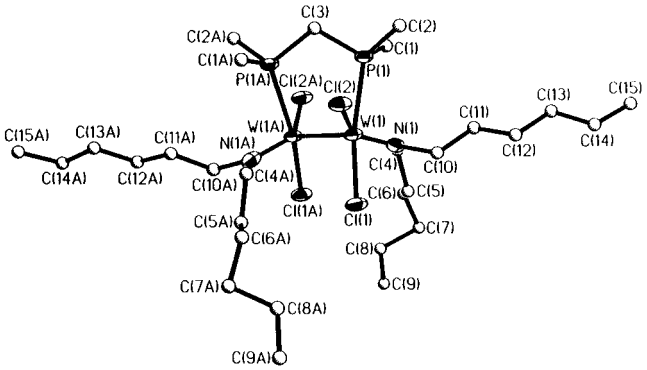

Figure 11. Perspective drawing of *cis,cis*-$W_2Cl_4(NHex_2)_2$(dmpm) (**5**). Only the major orientation of the hexyl chains is shown. Atoms are represented by thermal ellipsoids at the 40% probability level. Carbon atoms are shown as spheres of arbitrary radii.

that observed in $W_2Cl_4(NR_2)_2(PR'_3)_2$ molecules with monophosphines. A comparison of **2** with **1** reveals several changes in geometry and subtle changes in the molecular parameters. The geometric changes are obvious in the drawings shown in Figures 8a,b. This variation in geometry does not result in a significant change in the W−W bond length (0.006 Å) but does cause significant changes in W−P and W−Cl distances (Tables 2 and 4). The changes in W−P and W−Cl distances reflect the nature of the atoms that are trans to the P or Cl atom. The W(2)−P(2) bond distances differ by ca. 0.13 Å for **1** and **2**. Both W(2)−Cl(3) and W(2)−Cl(4) distances are also approximately 0.04 Å longer in **2** than in **1** due to the influence of the atoms trans to the atoms in question. The structural characterization of **4a,b** and **5** revealed little that is exceptional compared to **2**. The internal parameters for the $W_2Cl_4P_2N_2$ cores of these four complexes (Table 4) are, not surprisingly, very similar and, together with the previously reported $W_2Cl_4P_2N_2$ cores of $W_2Cl_4(NR_2)_2(PR'_3)_2$ molecules, form an interesting

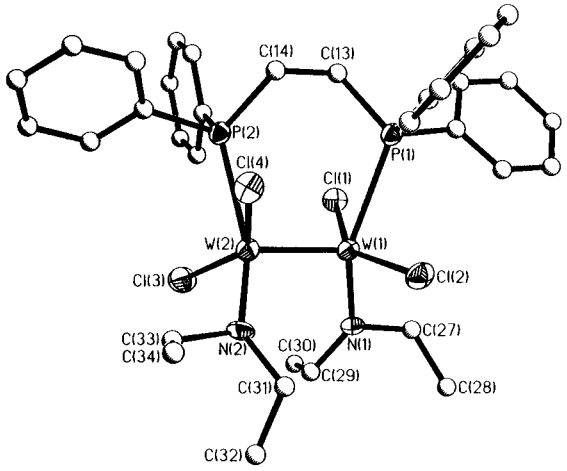

Figure 12. Perspective drawing of *trans,trans*-$W_2Cl_4(NEt_2)_2$(dppe) (**8**). Atoms are represented by thermal ellipsoids at the 40% probability level. Carbon atoms are shown as spheres of arbitrary radii. Phenyl rings are not labeled for clarity.

Table 6. Selected Bond Distances (Å) and Angles (deg) and Torsion Angles (deg) for *trans,trans*-$W_2Cl_4(NEt_2)_2$(dppe) (**8**)

W(1)−W(2)	2.3178(6)	W(1)−P(1)	2.659(3)
W(2)−P(2)	2.676(2)	W(1)−N(1)	1.910(7)
W(2)−N(2)	1.906(7)	W(1)−Cl(1)	2.378(2)
W(2)−Cl(4)	2.372(2)	W(1)−Cl(2)	2.360(2)
W(2)−Cl(3)	2.357(3)		

P(1)−W(1)−N(1)	150.8(2)	P(1)−W(1)−Cl(1)	75.33(8)
P(1)−W(1)−Cl(2)	82.19(8)	N(1)−W(1)−Cl(1)	91.1(2)
N(1)−W(1)−Cl(2)	97.4(2)	Cl(1)−W(1)−Cl(2)	147.17(9)
W(2)−W(1)−P(1)	103.71(5)	W(2)−W(1)−N(1)	104.7(2)
W(2)−W(1)−Cl(1)	104.67(6)	W(2)−W(1)−Cl(2)	103.69(7)
P(2)−W(2)−N(2)	158.7(3)	P(2)−W(2)−Cl(3)	85.19(8)
P(2)−W(2)−Cl(4)	76.49(8)	N(2)−W(2)−Cl(3)	94.6(3)
N(2)−W(2)−Cl(4)	91.1(3)	Cl(3)−W(2)−Cl(4)	141.74(9)
W(1)−W(2)−P(2)	96.08(5)	W(1)−W(2)−N(2)	104.3(2)
W(1)−W(2)−Cl(3)	106.89(8)	W(1)−W(2)−Cl(4)	108.21(7)

P(1)−W(1)−W(2)−P(2)	-38.48(7)	P(1)−W(1)−W(2)−Cl(4)	39.26(8)
N(1)−W(1)−W(2)−N(2)	-51.5(4)	N(1)−W(1)−W(2)−Cl(3)	48.0(2)
Cl(1)−W(1)−W(2)−P(2)	39.66(8)	Cl(1)−W(1)−W(2)−Cl(3)	-47.14(9)
Cl(2)−W(1)−W(2)−N(2)	50.1(3)	Cl(2)−W(1)−W(2)−Cl(4)	-45.88(9)

group of d^3-d^3 ditungsten compounds in a *cis,cis*-stereochemistry. The most obvious difference between them is the significant change in the torsional angles P−W−W′−P′ by switching from monophosphines to diphosphines. The complexes studied here with bridging diphosphines show torsional angles P−W−W′−P′ in the small range 36.3−37.3° (Table 5), while the corresponding values for $W_2Cl_4(NR_2)_2(PR'_3)_2$ molecules lie in the range 126.7−138.0°.

Compound 8. Crystals of **8** conform to the monoclinic space group $P2_1/n$ with four molecules per unit cell. There are also four toluene solvent molecules in the unit cell. Figure 12 displays a perspective drawing of the molecule in its entirety, and Figure 8c shows a view of the central portion down W−W

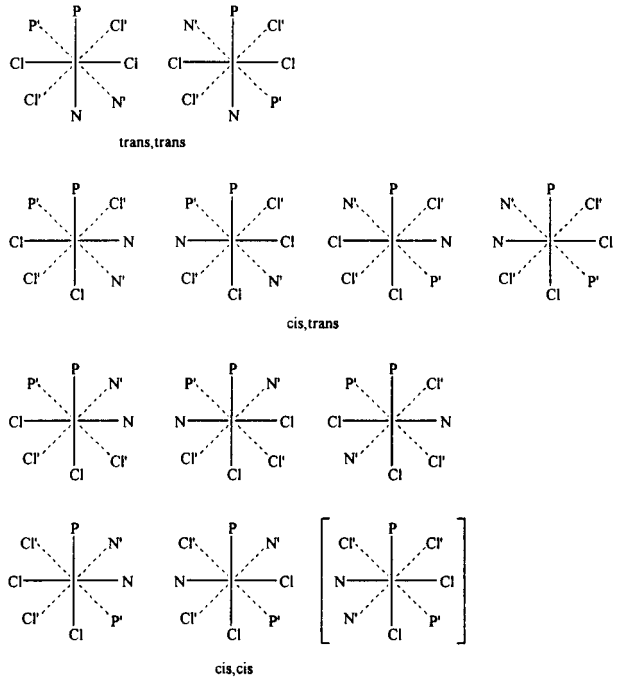

Figure 13. Schematic diagrams showing the 12 isomeric possibilities of $W_2Cl_4(NR_2)_2(PR'_3)_2$ molecules with a staggered conformation.

axis. Although orientational disorder of the W_2 unit has frequently been observed in *trans*-$W_2Cl_4(NHCMe_3)_2(PMe_3)_2$ molecules,[3] no indication of such a disorder can be observed in this structure. Compared with the previous structures **1** and **2** in Figure 8a,b, the obvious difference is that both phosphorus atoms are now arranged in trans positions to the two NEt_2 groups. The W−W bond distance of 2.3178(6) Å (Table 6) is characteristic of a W−W triple bond. The average W−Cl and W−P bond distances are 2.367(3) and 2.668(3) Å, respectively. The W−P distance is comparable to the corresponding distances observed in the trans WCl_2PN unit of all *cis,trans*-isomers mentioned above. Presumably, the trans influence order NEt_2 > PPh_2R accounts for the significant lengthening of the W−P distance in this case. The projection along the W−W axis, as shown in Figure 8c, shows the torsional angle P(1)−W(1)−W(2)−P(2) as 38.5° (Table 6).

Concluding Remarks

The preparation of $W_2Cl_4(NR_2)_2$(L-L) (L-L = bidentate phosphines) molecules by reaction of the $W_2Cl_4(NR_2)_2(NHR_2)_2$ type intermediate complex with a stoichiometric amount of L-L is reported here. For L-L = dmpm and dmpe, $^{31}P\{^1H\}$ NMR spectroscopic evidence suggests that three distinct isomeric species exist in solution, and they are the *trans,trans*-, *cis,trans*-, and *cis,cis*-isomers. The structural characterization of the *cis,trans*-compounds are of particular interest because these are the first examples of metal−metal-bonded complexes with such a stereochemistry.

In all the systems studied here, when the diphosphine ligands substitute NHR_2 of $W_2Cl_4(NR_2)_2(NHR_2)_2$, it is believed that the kinetic products are the *trans,trans*-isomers, as evidenced by $^{31}P\{^1H\}$ NMR spectra. However, we are still unsure of the exact mechanism for the formation of other isomers in this kind of reactions and a detailed explanation for this observation cannot be given at this time. Apparently, there should be some driving force, either kinetic or thermodynamic, that controls the fractions of each isomer in the product mixture. Detailed studies of the isomerization processes have to be pursued so as to determine what factors such as time, solvent, types of diphosphine used, or reaction conditions influence the processes and whether they are reversible.

On the other hand, out of the six possible geometrial isomers shown in Figure 1, only three of them (I, II, and IV) have been observed in all cases, irrespective of the bridging diphosphines and dialkylamido groups used. Presumably, a plausible explanation for this is the unfavorable interaction as a a consequence of steric repulsions between the PMe_3 and NR_2 groups in types III, V, and VI. It can be seen clearly that, for complexes of types I, II, and IV, there is no close contact between the N and P atoms in each case. This phenomenon can be further substantiated by the observation of only one type of isomer in the monophosphine system.[2] As illustrated in Figure 13, there are twelve isomeric possibilities in $W_2Cl_4(NR_2)_2(PR'_3)_2$ molecules with a staggered rotational geometry. Previous studies by us showed that $^{31}P\{^1H\}$ NMR spectroscopy indicated the absence of any *tran,trans*- or *cis,trans*-isomer in the reaction mixture.[2] It is evident from Figure 13 that all of the conformations except the known *cis,cis*-isomer (the one in brackets) exhibit highly unfavorable steric interactions between adjacent P atoms or between adjacent N and P atoms. The unique isomer thus formed is the one in which steric interactions between the bulky phosphine ligands or between PR'_3 and NR_2 groups are minimized. It is also noteworthy that close contact between two NR_2 moieties does not contribute much in determining the observed configurations of the molecules in question.

Acknowledgment. We are grateful to the National Science Foundation for financial support. We also thank the Department of Chemistry, The University of Hong Kong, for providing the diffractometer facilities for the X-ray data collection of compound **1** during the leave of absence of W.-Y.W. in Hong Kong.

Supporting Information Available: Nine X-ray crystallographic files, in CIF format, are available. Access information is given on any current masthead page.

IC961151Z